Precision Agriculture (2026) 27:97
https://doi.org/10.1007/s11119-026-10399-6

Optimising nitrogen application rate using grass coverage estimated at late autumn or early spring from RGB image analyses

Victor Rueda-Ayala[1] · **Tomas Persson**[2] · **El Houssein Chouaib Harik**[3] · **Christian Rueda-Ayala**[4]

Received: 6 March 2026 / Accepted: 3 June 2026

Abstract

Purpose Advanced remote sensing and imagery technology help to estimate variability in grass ley plant coverage (PC). Adjusted manure and fertiliser application rates can be derived according to this variability, by means of machine learning and advanced image processing. This study aimed to determine the effects of variable nitrogen (N) rate from manure and synthetic fertiliser application on a grass ley field experiment in southwestern Norway, thereby generating N rate recommendations. The effects on dry matter yield, N use efficiency, and forage nutritive value were determined.

Methods A field experiment was conducted in 2022-2023 and repeated in 2023-2024, estimating PC using digital processing of autumn and spring aerial images to determine fertiliser rates. Three fixed and two variable manure and mineral N rates were applied in early spring and after the first and second cuts. Forage dry matter yield (FDMY) and agronomic N use efficiecy (AgNUE) were evaluated over two seasons.

Results A low or variable N rate based on spring coverage led to FDMY and AgNUE comparable to high N rates. Spring and autumn coverage during the second season improved slurry application decisions, offering a valuable tool for grassland management. The N rate-response model effectively represented the nonlinear behaviour of FDMY, revealing a strong concave response to N rates, significant seasonal variations, and a notable flattening of the response in 2024. Predicted curves indicated that the most beneficial N application occurs in earlier cuts, as late-season applications showed diminished yield leverage under 2024 conditions.

Conclusion Image analysis can effectively support variable-rate fertiliser recommendations for perennial grasslands, although such approaches only improved N usage in one of two years. Whilst variable-rate application (VRA) is resilient during constrained regrowth years, interannual weather variability and seasonal conditions significantly influenced N responsiveness, indicating the necessity for calibrating cover-based models to enhance nutrient management efficiency under varying climate conditions.

Victor Rueda-Ayala and Tomas Persson contributed equally to this work.

Extended author information available on the last page of the article

Published online: 23 June 2026

Keywords Forage yield · Winter damage · Image analysis · Machine learning · Proximal sensing · Animal-dense regions · High latitudes

Introduction

Many regions in countries such as Norway, particularly in animal dense areas, experience a manure surplus. In these areas manure is often spread at levels exceeding plant nutrient demands (Nesme et al., 2015), which ultimately leads to inefficient plant nutrient use (Schoumans et al., 2014; Svanbäck et al., 2019). These practices are frequently associated with losses of nitrogen (N) and phosphorus (P), and negative environmental consequences (Miller et al., 2011). Such consequences include eutrophication of water bodies (Schoumans et al., 2014) and emissions of nitrous oxide, which contribute to climate change (Cameron et al., 2013). Inefficient use of plant nutrients is not just an economic loss at the farm level, but for the entire agricultural sector.

Animal dense regions in Northern Europe are dominated by sown perennial grasslands, which are usually harvested from the 2nd year after establishment and grown for at least 2 additional years before being ploughed and often rotated with cereal or other annual crops. Sown perennial grasslands are the main suppliers of ruminant feed, and are either cut 2–4 times per season and conserved as silage, or grazed (Helgadóttir et al., 2014). In grassland production, N use efficiency (defined by the amount of above-ground biomass produced per N input) depends on plant density, soil nutritional status and turnover, amount of applied nutrients, cutting regime and weather conditions (Höglind et al., 2020; Reuter et al., 2025). Beyond the amount of biomass produced, the nutritive characteristics of grass silage or grazed grass, including its protein content, neutral detergent fibres (NDF), starch, minerals, and its digestibility, are key to its value as ruminant feed (Shingfield et al., 2001). Thus, evaluations regarding the effect of N supply on sown perennial grasslands are often based on both the amount of produced biomass and the nutritive characteristics of the produced grass (Termonen et al., 2020). In cold temperate regions, harsh winters can affect the sward growth when the season commences, resulting in uneven coverage across the field (Rapacz et al., 2014).

Traditionally, plant nutrient input rates through fertilisers are determined after soil sampling and chemical analysis, and adjusted according to the yield potential based on previous yields and economic responses (Valkama et al., 2016; Wachendorf et al., 2004). Knowledge on field-specific soil and topography characteristics, climate conditions, farm data such as the quantity and types of animals, farm size and legal restrictions have been previously combined to construct a model that calculates grassland fertiliser requirements on a field basis and the amount of available fertiliser per farm (Kaim et al., 2025). However, this model does not consider intra-field variability in nutrient requirements. Furthermore, soil sampling, chemical soil analyses, and in-situ plant stand assessments to account for the intra-field variability are highly resource demanding, time consuming, and usually not economically feasible.

Recent advancements in remote sensing and imagery tools, combined with high technology manure spreading equipment (Fischer et al., 2025; Chen et al., 2025; Silva et al., 2023), highlight the potential to develop more precise and less resource demanding strategies for improved nutrient use efficiency in grassland production. Through these technologies it becomes possible to assess the within-field variation in plant density of crop and grassland fields (Borra-Serrano et al., 2019). The `Grasision`® tool was specifically developed to estimate plant cover (PC) from images acquired on grassland fields (Rueda-Ayala et al., 2019b). Previous studies compared within-field variable-rate application (VRA) of mineral N fertiliser, based on pasture growth and height assessed with a C-Dax pasture meter (https://pasture.io/c-dax-pasture-meter), with fixed N fertiliser rate on grazed, irrigated pastures in New Zealand (King et al., 2022). There, VRA resulted in a higher pasture growth rate than uniform N fertiliser application only one of five farms, and no significant differences in fertiliser use efficiency between the two treatments were observed. Moreover, variable-rate manure application (VRMA) based on soil P maps was developed and evaluated in annual cropping systems in Belgium (Zhang et al., 2022, 2024a).

Sown perennial grasslands in high latitude regions, which are frequently cut and conserved as silage, have another growth pattern that is characterised by periods of initial spring growth and re-growth after cutting (Smit et al., 2021; Peters et al., 2022), contrary to grazed pastures and cereal crops. Notably, the species and cultivar composition in grasslands of Northern Europe differ from grazed pastures in New Zealand (Helgadóttir et al., 2014; Chapman et al., 2018). In high-latitude regions, grasslands are often exposed to harsh winter conditions that negatively affect forage PC and subsequent yield (Rapacz et al., 2014; Persson et al., 2024). Consequently, N supply effects on the growth, yield, and nutritive characteristics of sown perennial grasslands may differ substantially from those observed in systems where VRA and VRMA strategies have been predominantly developed and tested.

Thus, VRMA practices must be developed and evaluated specifically for cut sown perennial grasslands. The main objective of this study was to adapt the `Grasision`® tool to provide N fertiliser recommendations for sown perennial grasslands under high-latitude conditions. The specific objectives were to assess how the timing of PC assessment influenced the accuracy of N rate recommendations, by comparing late autumn and early spring derived estimates, whilst accounting for overwintering effects on grass coverage. The study also sought to characterise continuous N rate-responses across three annual cuts over two consecutive years. It was hypothesised that N rate recommendations based on early spring PC are more accurate than those based on late autumn coverage, due to changes in sward structure that are caused by overwintering. It was further hypothesised that yield responses to increasing N rates are continuous but vary among cuts within a year, whilst remaining broadly consistent across years.

Methods

Experiment description and image acquisition

The experiment was conducted over two seasons at the NIBIO Særheim research station (Klepp Stasjon, Norway, lat. 58.76 N, long. 5.65 E), from October 2022 to September 2023 and repeated at the same site from October 2023 to September 2024, in an established sown grass ley. The monthly mean air temperature and accumulated precipitation for the study and reference periods at Særheim (Norwegian AgClimate Network, https://lmt.nibio.no/) are summarised in Table 1. Low, high, and no suppression levels of varying PC (due to plant death and growth reduction) across all fertiliser treatments were produced. The grass sward

Table 1 Mean monthly air temperature and accumulated precipitation at the NIBIO Særheim research station, for the experimental period October 2022 – September 2024 and the reference period 1991–2020

Month	Mean air temperature (°C)				Accumulated precipitation (mm)			
	2022	2023	2024	1991–2020	2022	2023	2024	1991–2020
January		3.0	0.42	2.3		201.3	156.8	149.8
February		4.3	3.0	1.7		137.2	178.1	109.3
March		2.3	4.8	3.1		125.4	118.3	88.4
April		6.5	6.4	6.4		35.2	72.0	72.6
May		8.8	14.7	9.6		51.1	48.4	72.7
June		14.6	12.3	12.3		59.2	134.2	75.4
July		14.2	14.5	14.6		198.5	151.1	104.7
August		14.5	14.9	14.9		155.9	237.8	141.7
September	11.5	14.3	13.2	12.5	151.8	188.5	154.5	148.6
October	8.6	7.8		8.7	193.9	91.4		167.6
November	4.4	3.5		5.3	215.7	84.9		155.7
December	2.0	1.9		3.1	100.6	124.8		156.6

damage was induced once on 20 October 2022, by rotary harrowing (high suppression) or mowing at a cut height of 1 cm (low suppression) on randomly distributed subplots within three repetition blocks (Fig. 1a). Colour images of the experimental field were obtained using a 21-megapixel camera mounted on an unmanned aerial vehicle (UAV) during aerial surveys conducted on 31 October 2022 and 2023, 28 February 2023, and 20 March 2024. Georeferenced orthomosaics of the whole field were reconstructed for each sampling season with the software `AgiSoft PhotoScan` (Agisoft, 2018).

Image analysis and fertiliser rate recommendation

The `Grasision`® image analysis tool was developed by NIBIO under the Norwegian research councils Milestone-project 'FORNY2020, Nr. 300567'. The tool uses machine learning (ML) algorithms to segment complex sward grass structures and estimate pixel coverage of living plants, dead plants, and bare soil from grassland colour images taken by UAV-mounted or tractor-mounted cameras (Rueda-Ayala & Höglind, 2019; Rueda-Ayala et al., 2019a, b). `Grasision`® was initially designed to recommend grassland renovation based on research data (Rueda-Ayala & Höglind, 2019). Gaussian mixture models and nearest centroid classifier, vegetation indices, and ML techniques were used following the procedure described below and in Rueda-Ayala et al. (2019a).

Processing pipeline and recommendation map generation.

The component of the Grasision model responsible for renovation decisions was adapted to generate recommendations for variable slurry and mineral fertiliser application rates (Fig. 2). Georeferenced red-green-blue (RGB) orthomosaics were processed through an automated pipeline to produce spatially explicit (site-specific) N application maps using slurry, in addition to grassland renewal maps. The pipeline (Fig. 2) was implemented as a sequence of shell scripts that invoke `GDAL` geospatial utilities and the Grasision image analysis tool. The workflow comprised five stages: coordinate reprojection, raster tiling, pixel-level clas-

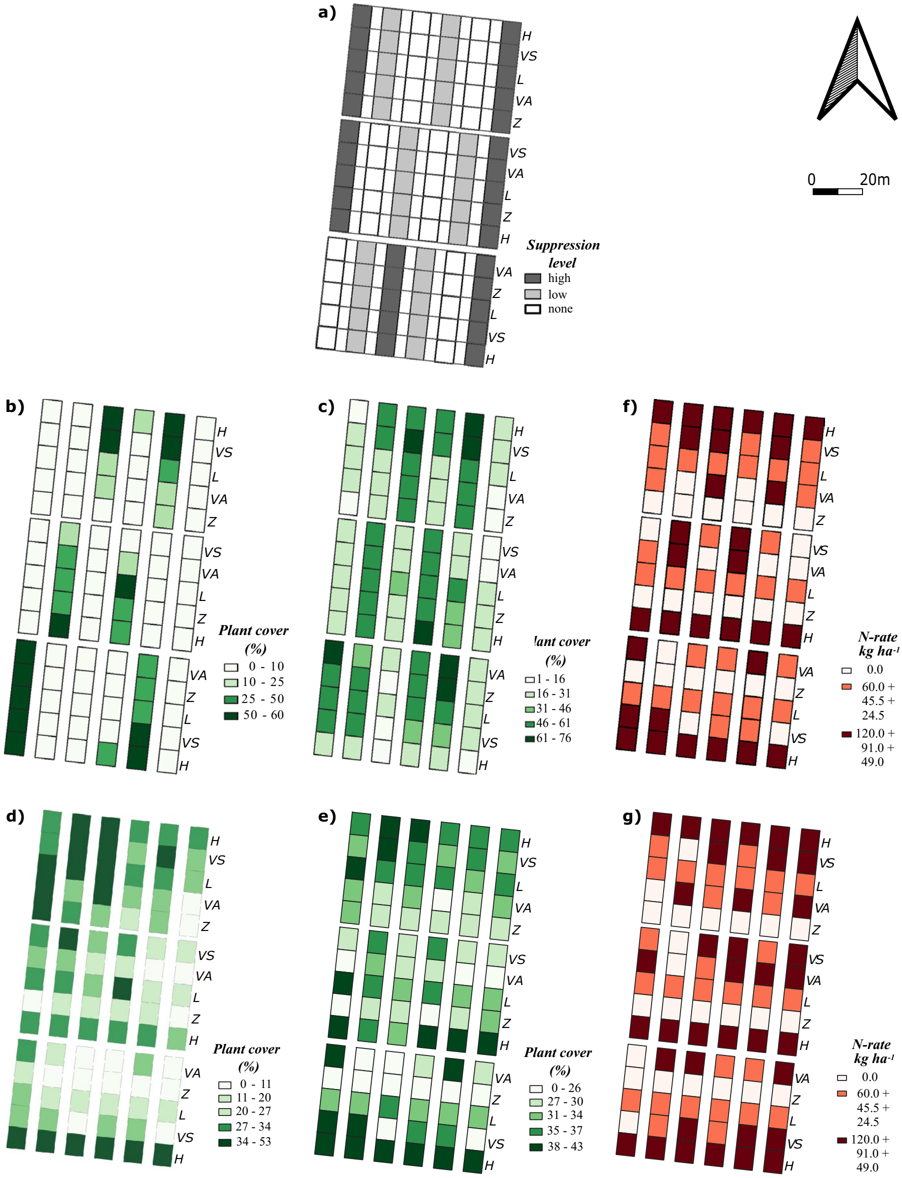

Fig. 1 Applied sward growth suppression treatments (**a**); estimated plant coverage (PC) autumn 31 October 2022 (**b**), spring 28 February 2023 (**c**), autumn 31 October 2023 (**d**), and 20 March 2024 (**e**); image-based fertiliser recommendation maps for 2023 (**f**) and 2024 (**g**). Fertiliser strategies in (**f**) and (**g**): *Z= Zero*, *L= Low*, *H= High*, *VA= VR.Autumn*, *VS= VR.Spring*. Actual N rate applied from slurry (0, 60, 120) and mineral sources after first cut (45.5; 91) and second cut (24.5; 49)

sification, georeferencing of classified tiles, and mosaic assembly, culminating in the generation of application maps.

Coordinate reprojection and tiling. The orthomosaics were delivered from `AgiSoft` in WGS-84 geographic coordinates (EPSG:4326), and they were therefore reprojected to

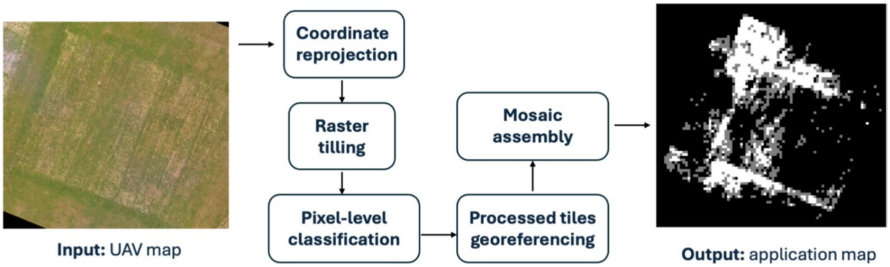

Fig. 2 Schematic overview of the image processing pipeline. The orthomosaic is reprojected, tiled, classified by the `Grasision`® tool, and reassembled into a field-wide site-specific recommendation map

Table 2 Ten per-pixel features extracted from the RGB orthomosaic and used as inputs to the neural network classifier

Colour space/index	Derived features
RGB	Red (R), Green (G), Blue (B)
YCbCr	Luminance (Y), Blue-chroma (Cb), Red-chroma (Cr)
CMYK	Cyan (C), Magenta (M), Key/Black (K)
CIVE	$0.441 \times R - 0.811 \times G + 0.385 \times B + 18.787$

UTM Zone 32 N (EPSG:25832) using `gdalwarp` to obtain a metric coordinate reference suitable for area-based analyses. The reprojected raster was subdivided into 100 × 100 pixel tiles. Each tile was accompanied by an `XML` file that stored the spatial extent and projection metadata, enabling the georeferenced mosaic to be reconstructed after classification.

Pixel-level vegetation classification. Segmentation of grass-sward structures was applied to tiles derived from the reconstructed orthomosaics. `Grasision`® classified each pixel into three categories: (i) living plants, characterised by high chlorophyll reflectance; (ii) dead plants, comprising senescent or dormant brown vegetation; and (iii) bare soil, where no vegetation cover was detected. Classification relied on a pre-trained multilayer perceptron that received a ten-dimensional feature vector per pixel, constructed from multiple colour-space transformations and the colour index of vegetation extraction (CIVE) (Table 2). Each pixel RGB values were converted into the `YCbCr` colour space (luminance `Y`, blue-difference chroma `Cb`, red-difference chroma `Cr`) and the `CMYK` colour space (cyan `C`, magenta `M`, key/black `K`), thereby yielding six additional channels. The original RGB values were retained, and the CIVE was computed (Kataoka et al., 2003). The CIVE emphasises green vegetation whilst suppressing soil and dry residue tones. Together with the multi-colour-space channels, it provides the neural network with complementary spectral information from a single RGB sensor. The model was applied in batches of 2000 pixels per tile to balance throughput and memory usage.

Neural network classifier and training. The multilayer perceptron was implemented in `TensorFlow (v2.4.1)` (Abadi et al., 2016) and `Keras (v2.4.3)` (Chollet et al., 2015). It mapped the ten-dimensional per-pixel feature vector to three mutually exclusive classes through a softmax output. The network consisted of two fully connected hidden layers (10 units each; ReLU activation) followed by a 3-unit softmax output layer (253 trainable parameters). Prior to training, the features were standardised using parameters estimated from the training set only and then applied unchanged to validation, test, and inference data. To avoid optimistic performance estimates caused by spatial autocorrelation, data were partitioned into independent training, validation, and test subsets using group-wise splitting by acquisition date and orthomosaic tile, ensuring that pixels from the same spatial unit did not occur in more than one subset; class proportions were preserved through stratification at the group level. The model was trained with categorical cross-entropy loss and the Adam optimiser using early stopping monitored on validation loss (min_delta = 1×10^{-3}; patience = 5; best weights restored). During inference, the classifier was applied tile-wise to generate per-pixel class labels, which were aggregated to compute tile-level living PC percentage for downstream recommendation mapping. Model training, tuning, and evaluation were conducted in `Python 3.8` using `Google Colaboratory` with GPU acceleration.

Recommendation map generation. After classification, the PC computed for each tile was translated into fertiliser management recommendations. For the N rate application map (from slurry and mineral fertiliser), three recommendation levels were defined based on the assumption that low living PC requires low amounts of N, whilst high PC requires more N; bare soil areas should not receive any fertiliser to avoid wasting nutrient resources (Table 3). The leaf area index (LAI) was an additional feature that was estimated for each tile as LAI = PC/100, thereby providing a continuous metric of canopy density alongside the discrete recommendation classes. Per-tile statistics, including living-plant, dead-plant, and bare-soil percentages together with the LAI and recommendation value were exported to a CSV file for data recording and formal statistical analysis.

Mosaic assembly and georeferencing. The classified tiles were converted into `GeoTIFF` format by re-attaching the `XML` metadata generated during the initial tiling step. All georeferenced tiles were subsequently merged into a single field-wide raster. The resulting recommendation map encoded the management classes as pixel values (0, 50, or 100) in a georeferenced `GeoTIFF` file that could be directly imported into a geographical information system and/or automated VRA equipment.

Validation with zonal statistics. To evaluate the correspondence between the recommendation map and observed field conditions, zonal statistics were computed in `QGIS`, version 3.40 (Qgis Development Team, 2025) for each experimental block (B1, B2, B3) and scouting date. Summary statistics (mean, median, and standard deviation) of recommendation pixel values were extracted per block and cross-referenced with both the suppression treatment (high, low, and none) and the amount of applied slurry (Fig. 1a). Through this approach, a block-level comparison between the remotely sensed PC and the expected response to the experimental treatments was possible. Blocks with high PC produced higher mean recommendation values (mean ≈ 64), reflecting increased slurry application recommendations. In contrast, blocks under high suppression treatments (*i.e.*, very low PC) showed markedly lower mean recommendation values (mean ≈ 10), in line with the minimal PC observed in the field. The Grasision classification component and associated thresholding logic produced spatially coherent and agronomically meaningful management recommendations.

Table 3 Slurry application recommendation thresholds based on living plant cover (PC) percentage. Application rate corresponds to the output map in Fig. 2, *High* = black pixels, *Low* = grey pixels, *Zero* = white pixels

PC	Recommendation value	Application rate
PC $> 60\%$	100	*High*
$28\% \leq PC \leq 60\%$	50	*Low*
PC $< 28\%$	0	*Zero*

Fertiliser application treatments

Five N fertiliser treatments were applied: three fixed rates at whole plot (45m × 7.5m) level, and two variable rates (VRs) adjusted site-specifically along 5 subplots (9m × 7.5m), totalling to the 45/m plot length. These VRs were based on the estimated PC (Fig. 1b, 1c, 1d, 1e). The N rate fertiliser map was produced with `Grasision`® (Figs. 1f, 1g). The three fixed treatments were evenly applied on each treatment plot, regardless of PC variation. The applied rates were i) *Zero*: 0 kg N ha^{-1}; ii) *Low*: 60 kg N ha^{-1} applied at the start of the growing season (April), 45.5 kg N ha^{-1} after the first cut (June), and 24.5 kg N ha^{-1} after the second cut (early August); and iii) *High*: 120 kg N ha^{-1} applied in April, 91 kg N ha^{-1} after the first cut, and 49 kg N ha^{-1} after the second cut. The *High* rate corresponded to typical N application rates in intensively grown grasslands in southwestern Norway. The VR in autumn (*VR.Autumn*) applied *Zero*, *Low*, and *High* rates based on October imagery. The VR in spring (*VR.Spring*) applied *Zero*, *Low*, and *High* rates according to estimated PC in February/March imagery. At the first application, N was partially supplied via cattle slurry (*low* = 26 kg N ha^{-1}; *High* = 52 kg N ha^{-1}), with the rest provided by mineral fertiliser (34 and 68 kg N ha^{-1}, respectively, from N 27-0-0).

Representative samples of the cattle slurry were analysed for nutritional contents by Eurofins Agro Testing Norway AS. In 2023, the slurry had a 4.1% dry matter content, pH 7.6 and 1000 kg t^{-1} volume weight. It included 2.7 kg total N t^{-1}, 1.31 kg ammonium-N t^{-1}, 0.33 kg P t^{-1}, 3.3 kg K t^{-1}, and 0.28 kg S t^{-1}. In 2024, the slurry had a 5.1% dry matter content, pH 7.6, and 1000 kg t^{-1} volume weight. It included 3.3 kg total N t^{-1}, 1.51 kg ammonium-N t^{-1}, 0.30 kg P t^{-1}, 7.4 kg K t^{-1}, and 0.39 kg S t^{-1}. In both years, the slurry was applied with a precision spreader, and rates were adjusted on the manure N-content calculated from chemical analyses and the NIBIO Nitrogen animal manure calculator (Husdyr N-Kalkulator, https://lmt.nibio.no/husdyrn/). After cut 1, N applied from slurry was 13 kg N ha^{-1} for the *Low* rate and 26 kg N ha^{-1} for the *High* rate; the rest was supplied from mineral sources (N 27-0-0), *i.e.*, 32.5 and 65 kg N ha^{-1}, respectively. After cut 2, all applied N came from mineral sources (N 27-0-0). Deficiencies of P and potassium (K) were avoided due to high application rates on all plots (except the *Zero* treatment), according to soil analyses.

Data collection and statistical analysis

The field was cut three times in both 2023 (31 May, 2 August, and 21 October) and 2024 (12 June, 31 July, and 23 September). Areas measuring 1.5 m × 7.5 m in the centre of each subplot were harvested and weighed. From the harvested material, samples of 0.8–1.0 kg fresh weight were dried at 60 °C for 48 h and weighed to determine the forage dry matter yield (FDMY). Total FDMY per year was calculated by the yield of all three cuts. The agronomic N use efficiency (AgNUE) (Congreves et al., 2021) indicated how efficiently N was used to effectively produce harvestable forage matter. AgNUE was calculated for the annual yield response and fertilization applied with the formula AgNUE $= [(\text{Annual FDMY} - \text{Annual Zero})/\text{Annual kg N applied}]$. The nutritive value, including the concentration of crude protein (%) and neutral detergent fibre NDF (%), and the digestible organic matter (%) in the dry matter (DOMD) of the grass samples were analysed using Near-infrared spectroscopy (NIRS). Above-ground plant samples were cut using a Wintersteiger Hege 44. Approximately 50 g of the dried and cut plant material were ground using a Foss Cyclotec mill to obtain a final particle size of 0.1 mm. Spectral signals for the cut and ground samples were obtained using a NIR Foss NIRS DS 2050 F spectrometer (Foss AS, Hillerød, Denmark). This spectrometer measures the adsorbed light spectrum from 850 nm to 2500 nm at a 0.5 nm interval. The registered spectral signals were compared with pre calibrated models representing forage grass leys in Norway to assess the three nutritive value attributes. In total, crude protein, NDF concentration, and DOMD were determined for samples from cuts 1 and 2 in 2023 and the cut 1 in 2024.

All statistical analyses were conducted in `R`, version 4.5.2 – "[Not] Part in a Rumble" (R Core Team, 2025) using the `nlme` package for linear mixed-effects modelling (Pinheiro et al., 2023). Two mixed-effects models were fitted to compare the N management strategies at the field level (Strategy-decision model) and estimate the N response (N rate-response model). Spatial information was incorporated via exponential spatial correlation structures, and heteroscedasticity was modelled with variance-covariate functions.

Strategy-decision model

To evaluate the agronomic performance of N management strategies across years and cuts, a linear mixed-effects model (1) was fitted with per-cut FDMY (t ha^{-1}) as the response variable. The same model was applied to evaluate the response of the grass nutritive value parameters measured via NIR-analysis, namely crude protein (%), NDF (%), and DOMD (%). The model was fitted via the restricted maximum likelihood (REML). The fixed-effects structure included the full factorial interaction among N management strategy (N_{str}), *Year*, and *Cut*, together with *Suppr* (grass suppression) as a baseline covariate:

$$Y_{bsrcy} = \mu_{(N_{str} \times Year \times Cut)} + \beta_{Suppr} + u_b + v_{b(s)} + w_{b(s)(r)} + \varepsilon_{bsrcy} \tag{1}$$

Here,

- Y_{bsrcy} is the response variable FDMY,
- $u_b \sim N(0, \sigma^2_{BL})$ is the random effect of block (*BL*),
- $v_{b(s)} \sim N(0, \sigma^2_{BL:N_{str}})$ is the random effect of strip (N_{str}) nested within block,
- $w_{b(s)(r)} \sim N(0, \sigma^2_{subplot})$ is the subplot-level random effect (*subplot*),

- ε_{bsrcy} are residuals with a spatial correlation structure.

Spatial autocorrelation among residuals was modelled using an exponential correlation function based on subplot centroid coordinates:

$$\mathrm{cor}(\varepsilon_i, \varepsilon_j) = \exp\left(-\frac{d_{ij}}{\phi}\right),$$

with a nugget effect to account for micro-scale variability. Residual heteroscedasticity was accommodated using a combined variance structure:

$$\mathrm{Var}(\varepsilon) = \sigma^2_{Cut}\, \sigma^2_{Year}\, \sigma^2_{N_{str}},$$

implemented as a product of `varIdent` structures. Adjusted marginal means for each $N_{str} \times Year \times Cut$ combination were obtained with the `emmeans` package (Lenth, 2023). Annual treatment FDMYs were computed as linear combinations of cut-level marginal means, enabling treatment comparisons and calculation of N use and N savings.

Nitrogen rate-response model

To estimate the functional response of yield to the continuous N rate applied at each subplot and cut, a nonlinear rate-response mixed model (2) was used. N rate (*NR*) was modelled using a natural cubic spline with two degrees of freedom:

$$Y_{bsrcy} = f_{spline}(NR \times Year \times Cut \times PC + \beta_{Suppr} + u_b + v_{b(s)} + w_{b(s)(r)} + \varepsilon_{bsrcy} \quad (2)$$

Here,

- Y_{bsrcy} is the response variable FDMY,
- $f_{spline}(NR)$ allows nonlinear yield response to N rate,
- *Year*: different response shapes across years,
- *Cut*: cut-specific modifications of the N response,
- *PC*: vigour-dependent shifts or shape changes via representative plant cover percentiles.

The random-effects structure ($BL/N_{str}/subplot$) and spatial autocorrelation (*corExp*) were identical to model (1). Residual variance was modelled with stratum-specific variances for each $Year \times Cut$ combination using `varIdent`. Predicted response curves with 95% confidence intervals (95%-CI) were obtained with `emmeans` and evaluated over a grid of N rates and representative PC percentiles of plant vigour (low ~25%, medium ~50%, and high ~75%). Marginal N responses ($\Delta Y/\Delta N$) and break-even thresholds were computed from finite differences of the predicted spline curves. Marginal means were pairwise contrasted and adjusted with the Tukey HSD ($\alpha = 0.05$) method. Treatment comparisons with statistical differences belonged to different Tukey groups and were marked with different letters.

Results

Forage yield response to N fertiliser strategies

The strategy-decision model (1) to determine performance of N management across years and cuts converged successfully and proved to be a good fit (Table 4). Variance components indicated negligible variability at the block level, moderate variation at the strip level, and greater variability at the subplot level. Spatial dependence was limited, with a short correlation range and a non-negligible nugget effect, indicating limited spatial dependence and the presence of fine-scale variability. Residual variance differed across cuts, years, and treatments, with higher variability associated with VRA strategies and lower variability in later cuts and in 2024. Fixed effects were dominated by a strong *Year:Cut* interaction (Fig. 3). Compared with 2023, yields in 2024 declined significantly at cuts 2 and 3. Differences among fertiliser treatments were the greatest early in the growing season and diminished

Table 4 Summary of strategy-decision model (1) fit, variance components, spatial structure, and relevant fixed effects

Parameter	Estimate
Model fit	
AIC	1132.6
Log-likelihood	−523.3
Random effects (SD)	
Block (BL)	0.005
Strip (N_{str} within *BL*)	0.060
Subplot (subplot within N_{str} within *BL*)	0.166
Residual	0.966
Spatial correlation	
Range (ϕ, m)	3.80
Nugget	0.649
Heteroscedasticity multipliers	
Cut 2	0.60
Cut 3	0.37
Year 2024	0.55
Low	1.02
High	1.39
VR.Autumn	2.05
VR.Spring	2.01
Fixed effects (estimate, p-value)	
Year 2024	$0.76\ (p = 0.0015)$
Cut 2	$1.89\ (p < 0.001)$
Cut 3	$-0.72\ (p = 0.0018)$
Year 2024 × Cut 2	$-4.32\ (p < 0.001)$
Year 2024 × Cut 3	$-1.91\ (p < 0.001)$
VR.Autumn × Year 2024	$1.57\ (p = 0.004)$
VR.Spring × Year 2024	$1.19\ (p = 0.027)$
Low × Cut 3	$-1.33\ (p = 0.0001)$
High × Cut 3	$-1.11\ (p = 0.0044)$

toward cut 3. In particular, the advantage of fertilized treatments over the *Zero* treatment decreased by cut 3. VRA strategies demonstrated improved performances in 2024 at cut 1, whereas fixed-rate treatments (*Low* and *High*) were relatively stable across years. Adjusted marginal means of annual FDMY confirmed these patterns (Fig. 4a). In 2023, the fixed *Low* and *High* treatments achieved the highest yields, whilst VRA treatments were lower. In 2024, *VR.Spring* and *VR.Autumn* produced yields statistically comparable to the *High* treatment despite substantially lower N inputs.

Nitrogen use efficiency

The total amount of applied N (Fig. 4b) was reflected in the contrasting AgNUE responses (Fig. 5). The *Low* treatment was consistently ranked among the most efficient, whereas *High* was the least efficient. Fixed rates in 2023 outperformed VRA strategies but in 2024 VRA matched the *High* treatment whilst using 42–50% less N. Moreover, VRA strategies achieved comparable annual FDMY with approximately 110–130 kg N ha^{-1} less input on average (Fig. 4b), showing the highest efficiency in 2024 (Fig. 5). These results highlight

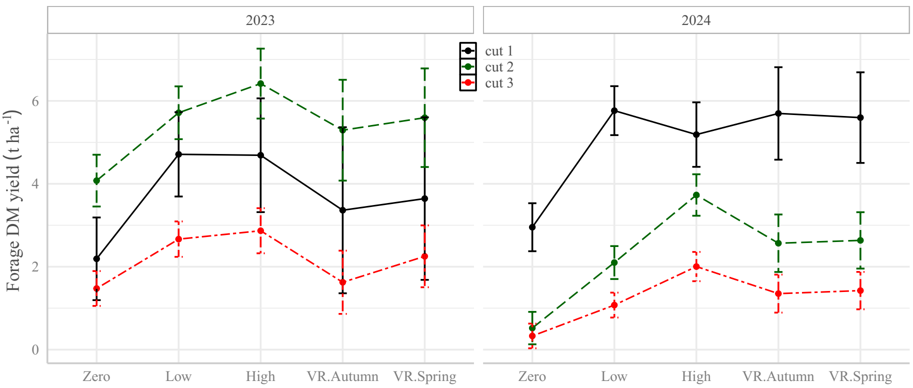

Fig. 3 Adjusted marginal means of FDMY per fertilisation treatment at 3 cuts per growing season (2023 and 2024) with 95%-CIs (thin vertical lines). Statistical differences occur when CIs do not overlap

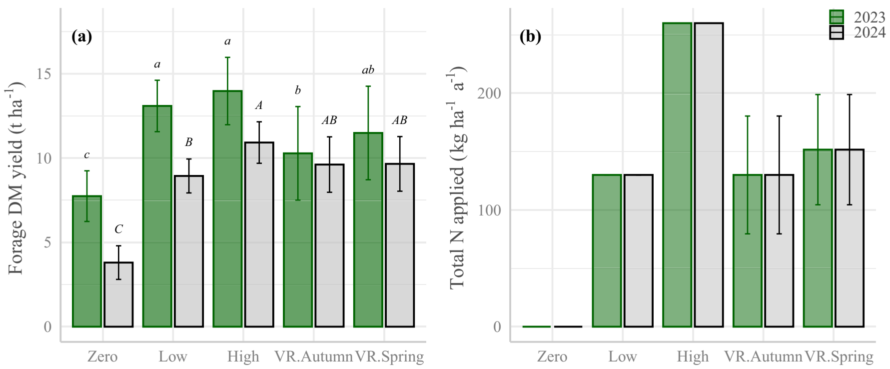

Fig. 4 Adjusted marginal means of FDMY per fertilisation treatment and year **(a)** with 95%-CIs (thin vertical lines). Italic letters indicate the adjusted Tukey comparisons on marginal means (lower-case = 2023; upper-case = 2024), where common letters are assigned to the same groups. Total N fertiliser applied per growing season (**b**); vertical lines: standard deviations due to the variable-rate used

the potential of VRA strategies to maintain productivity whilst reducing N inputs, particularly under less favourable regrowth conditions. Model (1) did not include PC as preliminary analyses did not indicate a consistent effect on AgNUE at the cut level.

Nitrogen rate response

The N rate-response model (2) provided a good fit to the data (Table 5) and captured the nonlinear FDMY response using a natural cubic spline (*ns*(*Nrate*, 2), Fig. 6). Variance components indicated minimal block-level variability, with greater variation at the strip and subplot levels. After accounting for random effects and fixed structure, residual spatial dependence was negligible. Residual variance remained heteroscedastic across *Year:Cut* combinations; variability decreased at later cuts, being lowest in 2024 cut 3. These results maintained consistency with reduced regrowth under unfavourable conditions. Fixed effects revealed a clear, nonlinear (concave shape) response of FDMY to N rate (Fig. 6). Seasonal effects were again

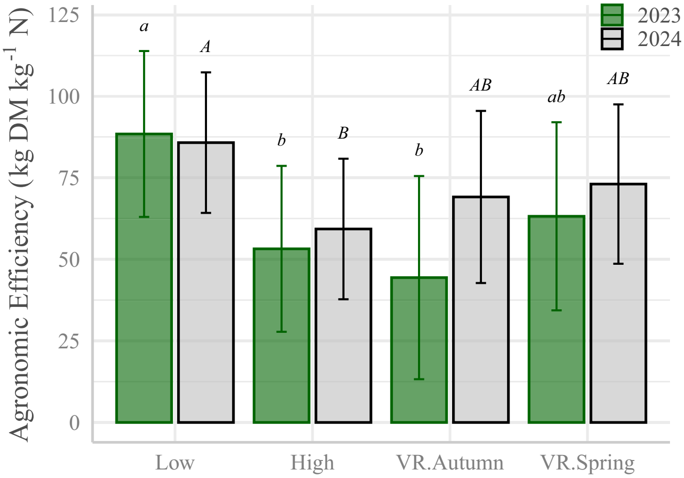

Fig. 5 Adjusted marginal means of the annual agronomic N use efficiency (AgNUE) (kg DM yield kg^{-1} N) per fertilisation treatment and year. Thin vertical lines indicate 95%-CIs. Italic letters indicate the adjusted Tukey comparisons on marginal means (lower-case = 2023; upper-case = 2024), where common letters are assigned to the same ranks

strong, with substantial yield reductions in 2024 at cuts 2 and 3 relative to the early-season baseline. Interactions between N rate and year indicated a flatter response curve in 2024, particularly at later cuts, making reduced yield gains from additional N under adverse seasonal conditions evident. PC exhibited a small positive main effect on FDMY, indicating a modest upward shift in yield level. However, non-significant interactions of PC and N-rate spline suggest that PC influenced the general yield without altering the shape of the N response.

Predicted N rate-response curves by Year and Cut (Fig. 6) showed: (i) a steep rise and plateau around ~50–80 kg N ha^{-1} at cuts 1–2, diminishing yield thereafter; (ii) very limited marginal response at cut 3, particularly in 2024; and (iii) only modest vertical separation among vigour percentiles (P25, P50, P75), confirming that vigour shifts the level more than the shape of the N response. In practice, most of the profitable N response occurs in earlier cuts; late-season N has little yield leverage in 2024 conditions.

Effects on nutritive value

Fertilisation with N showed pronounced effects on crude protein (%), NDF (%), and DOMD (%) across treatments, years, and cuts (Table 6). In cut 1 of 2023, crude protein strongly increased with N rate, from 9.9% in *Zero* to 16.3% in *High* N rate, whilst *VR.Autumn* and *VR.Spring* showed intermediate values. A mirrored gradient was observed for NDF, going from 41% for *Zero*-N to 48.6% for *High*-N. DOMD demonstrated an inverse pattern, declining from 83.8% to 77.4% for treatments *Zero* and *High*, respectively. Similar trends were observed for cut 1 of 2024, but with lower absolute crude protein and DOMD values and higher NDF values than 2023, consistent with the climatic differences between years. In 2024, the *High* N rate resulted in the highest crude protein content (14.1%), whereas *VR. Spring* exhibited slightly elevated NDF (55.6%) relative to the other treatments. Cut 2 of 2023 indicated reduced responsiveness to N fertiliser. Although crude protein increased

Table 5 Summary of N rate-response model (2) fit, variance components, spatial structure, and relevant fixed effects.

Parameter	Estimate
Model fit	
AIC	1309.5
Log-likelihood	-605.8
Random effects (SD)	
Block (*BL*)	0.001
Strip (N_{str} within *BL*)	0.584
Subplot (subplot within N_{str} within *BL*)	0.237
Residual	0.916
Spatial correlation	
Range (ϕ, m)	≈ 0.11
Nugget	≈ 0.001
Heteroscedasticity (Year × Cut multipliers)	
2023 Cut 2	0.81
2023 Cut 3	0.61
2024 Cut 1	0.94
2024 Cut 2	0.64
2024 Cut 3	0.24
Fixed effects (estimate, p-value)	
N rate (ns term 1)	$2.57 (p < 0.001)$
Year 2024	$3.49 (p < 0.001)$
Cut 2	$2.80 (p < 0.001)$
PC	$0.042 (p < 0.001)$
Year 2024 × Cut 2	$-5.67 (p < 0.001)$
Year 2024 × Cut 3	$-3.55 (p < 0.001)$
N rate (ns term 2) × Year 2024	$-1.86 (p = 0.001)$
Year 2024 × PC	$-0.073 (p < 0.001)$
Cut 2 × PC	$-0.033 (p = 0.003)$
Year 2024 × Cut 2 × PC	$0.045 (p = 0.003)$

with higher N rate (*Zero*: 7.2%; *High*: 11.2%), treatment differences were less pronounced compared with cut 1. DOMD remained high (65–71%), with slightly lower values of *VR. Spring* than the fixed N-rate treatments. NDF differences were smaller compared with cut 1, reflecting the variability expected at each cut. The Tukey groupings indicated a clear separation among N rates in 2023 and 2024 for cut 1, whereas fewer differences occurred in cut 2. The nutritive value results of different N rates influenced more percentages of forage crude protein, NDF, and DOMD at cut 1 each year, and the differences were less obvious later in the season. Nutritional characteristics for variable N rates were intermediate, corresponding to the intermediate N supply levels that were applied.

Discussion

Fixed versus variable N rate strategies

Across both modelling approaches, *i.e.*, strategy-decision and N-rate response, the findings in this study show a strong conditioning of N responsiveness in sown grasslands to the

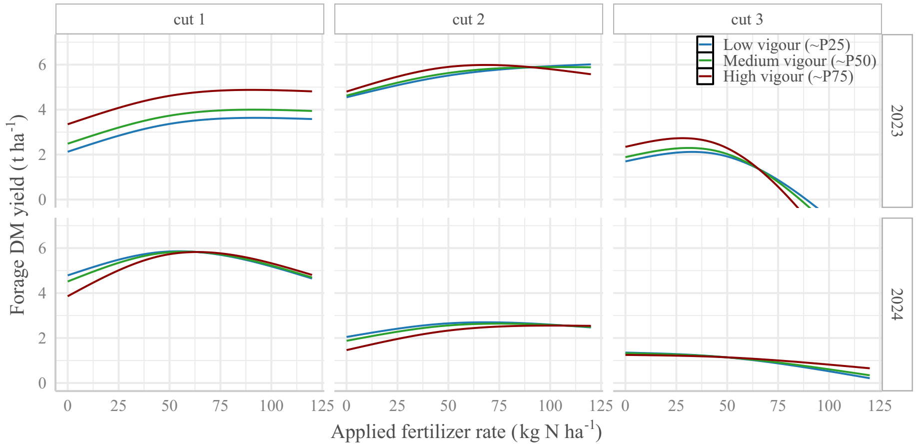

Fig. 6 Predicted N rate-response curves of FDMY (adjusted marginal means with 95%-CIs) by `Year` and `Cut` at three plant-cover percentiles (P25/P50/P75), illustrating diminishing yield and weak late-season response in 2024

Table 6 Adjusted marginal means of percentages of nutritive value parameters assessed via NIR-spectroscopy, crude protein, neutral detergent fibres (NDF), and digestibility (DOMD); standard errors (SE) shown in parentheses. Common italic letters show values in the same Tukey group: lowercase = 2023, uppercase = 2024

Treatment	Year	Cut	Crude protein (%)	NDF (%)	DOMD (%)
			Adjusted mean (± SE)		
Zero	2023	1	9.9 (0.6) *c*	41.0 (1.6) *c*	83.8 (1.4) *a*
Low	2023	1	11.9 (0.6) *bc*	46.6 (1.6) *ab*	79.0 (1.4) *bc*
High	2023	1	16.3 (0.8) *a*	48.6 (1.7) *a*	77.4 (1.5) *c*
VR.Autumn	2023	1	10.9 (0.8) *bc*	44.2 (1.7) *b*	81.4 (1.5) *ab*
VR.Spring	2023	1	12.7 (0.8) *b*	44.7 (1.8) *ab*	80.8 (1.5) *abc*
Zero	2024	1	7.5 (0.6) *C*	51.5 (1.8) *B*	73.8 (1.5) *A*
Low	2024	1	9.9 (0.6) *B*	53.8 (1.7) *AB*	71.1 (1.4) *AB*
High	2024	1	14.1 (0.7) *A*	53.9 (1.7) *AB*	70.8 (1.4) *AB*
VR.Autumn	2024	1	10.5 (0.7) *B*	54.3 (1.6) *AB*	70.9 (1.4) *AB*
VR.Spring	2024	1	12.1 (0.7) *AB*	55.6 (1.7) *A*	69.5 (1.4) *B*
Zero	2023	2	7.2 (0.2) *c*	56.0 (1.2) *ab*	67.6 (1.2) *ab*
Low	2023	2	9.5 (0.3) *b*	54.4 (1.2) *ab*	69.6 (1.2) *ab*
High	2023	2	11.2 (0.3) *a*	52.1 (1.2) *b*	71.0 (1.2) *a*
VR.Spring	2023	2	8.9 (0.5) *bc*	57.2 (1.1) *a*	65.4 (1.2) *b*
VR.Autumn	2023	2	8.4 (0.5) *bc*	55.9 (1.3) *ab*	67.8 (1.2) *ab*

yearly weather patterns and within-season regrowth potential. The strategy decision model suggested favourable early-season growing conditions in 2023 which favoured a strong yield response to fixed *Low* and *High* N rate treatments to achieve the highest annual yields. Contrarily, important yield reductions for cuts 2 and 3 in 2024 limited the agronomic benefit of additional N. Multi-year studies have found strong seasonal effects on VRs performance and profitability: prescriptions derived from early-season vigour –via (normalised difference vegetation index) NDVI data– outperformed historical yield in favourable seasons, whereas the opposite occurred when early conditions deteriorate later in the year (Lee et al., 2025). Sensor-based derived VR N-application typically reduces N inputs and improves N use efficiency without yield losses, although these year-dependent benefits are not universal across all sites/years (Hagn et al., 2025; Stamatiadis et al., 2018). Variable N distribution with UAVs in wheat reported substantial reductions in applied N (5–40%) with inconsistent yield gains. Those findings reinforce idea that the N use efficiency improvements acquired through precision agriculture technologies are due to N savings rather than increased yield (Argento et al., 2021).

The nonlinear N rate-response model (2) demonstrated steep yield gains at low-to-intermediate N, followed by a plateau at higher rates. This behaviour is consistent with asymptotic curves of N responses in cereal and forage systems, with low global N use efficiency ($\approx 33\%$) and substantial losses when supply exceeds crop demand (Raun & Johnson, 1999). The strong *Cut* : *Year* interactions in this study align with well-established seasonal patterns in grassland systems. Spring N applications generate larger yield responses, whereas late-season or drought-affected regrowth exhibits little responsiveness (Sun et al., 2008). The minimal marginal response observed at cut 3 in 2024 is comparable with reports of reduced N effectiveness in late harvests or under moisture stress. Percentiles of PC (P25, P50, P75) shifted the position of the response curve without altering its shape (Fig. 6). This effect was evident in a sensor-based N rate management study, in which NDVI and related vigour indices were the most informative early in the season, with declining predictive power as the crops matured (Hnizil et al., 2024; Vizzari et al., 2019). Moreover, the PC $\times$ N rate interactions in the present study were weak. Different functional N-response curves for sensor-guided fertiliser management trials in wheat did not occur by NDVI zones, although NDVI may alter intercepts or optimal application timing (Mitra et al., 2023).

Across all tested N rate strategies, the fixed *High* N treatment consistently produced the highest yields, especially in favourable seasons (Table 1), whilst VR strategies showed greater resilience under constrained regrowth conditions. Other multi-site winter wheat evaluations have found that sensor-based recommendations captured the yearly variability in economically optimal N rate (EONR) more effectively than static or uniform systems (Bushong et al., 2016; Pinto et al., 2025). In 2024, VRs produced annual yields comparable with *High* rates whilst applying roughly 42–50% less N. Other studies also identified that VRs maintain yield whilst substantially reducing inputs (Hagn et al., 2025; Stamatiadis et al., 2018). From a management perspective, this study supports three principles of precision N management, namely (i) most profitable and agronomically efficient N responses arise early in the season; (ii) late-season N applications rarely improve yield under environmental or climatic stress; and (iii) the greatest advantage of VRs is adaptation to temporal variability and reduction of unnecessary inputs instead of exploiting site-specific spatial differences alone (Lee et al., 2025; Raun & Johnson, 1999). For forage systems that are experiencing increasing climatic variability, the capacity of VR to maintain yield whilst lowering total N input offers environmental advantages (although these are not directly quantified in this study) and makes it a robust management strategy.

Previous research on VRA or VRMA regimes is dominated by studies on annual field and horticultural crops for human consumption (Pawase et al., 2023). The differences in growth patterns and harvest regimes between these crop types and perennial grasslands complicate the comparison with the findings presented here. Unlike results from grazed pastures in New Zealand (King et al., 2022), this study demonstrated improved N use efficiency with VRMA based on ground PC. Additionally, a slightly larger wheat and barley yield was observed for manure application that was adjusted to the soil P status (Zhang et al., 2024a, b). In a sorghum field trial under organic farming in Tuscany, Italy, a variable N-rate strategy adjusted by integrating sensor-acquired NDVI and agronomic inputs achieved higher N use efficiency and N savings than a traditional fixed rate (Silva et al., 2024). However, a new NDVI acquisition 1.5 months after manure application was not carried out in that study. Nevertheless, these results evidently demonstrate that variable N-rate application is highly dependent on both the type of crop and which growth indicator is assessed.

The lack of consistent effects from VRA and VRMA across seasons in the present study may be linked to the fact that the *High* rate was already delivering substantially higher N levels than the grass plants demanded, which was shown by the N rate forage yield response analysis. Furthermore, this assumption was supported by the differences in nutritive value attributes (Table 6), especially NDF and DOMD, between the fixed *High* and *Low* N rate treatments. VRMA effects may differ or be more pronounced in more extensive silage grass production systems with lower N rates. The larger difference in crude protein than in NDF concentration and DOMD between the fixed *High* and *Low* N rates ins consistent with previous grassland studies in high latitude regions, which have reported a stronger positive effect on crude protein than DOMD (Termonen et al., 2020). Apparently, N supply is more critical in feeding systems where protein is primarily supplied through forage than systems which use feed concentrate. The lower protein concentration in the VRA treatments than in the *High* fixed rate may negatively qualify VRA in terms of production security in feeding systems where forage is the main crude protein source. However, in this study nutritive value was only analysed for cuts 1 and 2 in 2023 and cut 1 in 2024 and manure application might have affected the forage nutritive value in the subsequent cuts differently.

The observed larger crude protein concentration with *High* N aligns with established physiological mechanisms whereby N availability stimulates protein synthesis and leaf growth in forage grasses (Ali et al., 2025; Anas et al., 2020). The contrary behaviour of NDF increasing and DOMD declining under high N supply reflects a typical trade-off: as the canopy becomes richer in N and more productive it accumulates greater structural biomass, leading to a higher proportion of cell-wall material relative to soluble components (Sigua et al., 2013). The weaker response of nutritive value traits in cut 2 is consistent with mid- and late-season regrowth, being more strongly constrained by water and heat stress, lower physiological N demand, and declining leaf-to-stem ratios (Govindasamy et al., 2023). These conditions reduce N uptake efficiency and the marginal quality benefits of additional N. Furthermore, the generally lower crude protein and DOMD, and higher NDF in 2024 relative to 2023 may reflect interannual climatic influences on N assimilation and fibre accumulation.

VR strategies produced intermediate crude protein and DOMD, which could be tracked to their intermediate N rates. In agronomic terms, VRs distribute N spatially but do not necessarily increase marginal N use efficiency, unless N is reduced in low-response zones (Ali et al., 2025; Kapoor et al., 2025). The somewhat higher NDF in *VR.Spring* in 2024 demonstrates the critical challenge associated with adjusting the N timing relation to crop growth stage for optimising both quality and yield potential. Together with yield and AgNUE results, the nutritive value at high N rates elevated crude protein but also increased NDF and reduced DOMD, whilst moderate N rates balanced quality and efficiency. The seasonal decline in responsiveness (*i.e.*, cut 2), highlights the importance of aligning N application with the periods of highest physiological and environmental potential for quality gains.

Uncertainties associated with weather variability and plant cover

The fact that N usage in 2023 was significantly lower for *VR.Autumn* than for *VR.Spring* but not in 2024 could be due to differences in temperature, precipitation, and snow cover duration between the two winters (https://lmt.nibio.no/), which thus affected the grass survival to varying degrees. Moreover, ambient light fluctuations and bidirectional reflectance can increase noise and index variability, affecting estimation of vegetation indices from RGB/CIR UAV imagery, especially under variable sunlight conditions. These conditions must be carefully controlled or corrected to enable reliable assessments (Arroyo-Mora et al., 2021; Rasmussen et al., 2016). Some studies using vegetation indices for site-specific N management approaches have relied on colour images taken under clear-sky, well-illuminated windows early in the season for reliable development of indices and decision models (Gnädinger & Schmidhalter, 2017; Jiang et al., 2019; Roth & Streit, 2017). Further testing of `Grasision`® should consider a larger variation in winter conditions, *e.g.*, by including fields from different climate zones or using species and cultivars with varying levels of winter hardiness to improve its ability to manage winter effects on plant ground cover estimation.

Differences in the weather between the two growing seasons could have also affected the results, notably by its effects on manure N mineralisation, losses, and availability which vary with weather conditions (Bhogal et al., 2016; Louro et al., 2013). The precipitation in June in 2023 was approximately 50% lower than in June 2024, which may explain the effect differences of manure application strategies on cut 2 for FDMY and N usage. The relatively better effect of VRs compared with fixed strategies during conditions with overall lower yield (*e.g.*, 2024 v. 2023) suggests that VRs performs more reliably even when climatic conditions forecast lower yield potential. Furthermore, this difference in VR effect also resulted in a lower FDMY variation between the two years compared with the fixed rate treatments, which suggests that VRs compensate for varying precipitation patterns.

Future studies

The effects of VRA/VRMA based on PC derived from colour UAV imagery require further investigation, particularly in grasslands and ruminant-based farming systems. The diminishing yield response to N at high supply levels suggests that applying lower maximum manure rates than those used in this study may help to reduce the masking effects of surplus N inputs. The influence of overwintering on remote-sensing-based N recommendations should be evaluated across multiple fields with varying winter severity. Such assessments are also needed to determine the feasibility of generating N application maps early in the season to support management planning. Multi-site experiments would further help to assess the consistency of the effects reported here across a broader range of soil types and botanical compositions representative of forage-grass systems in high-latitude regions. Furthermore, studies incorporating controlled irrigation could clarify how water availability interacts with VRMA. Considering these efforts together could support the development of integrated nutrient budgets (N, P, K) that improve manure management efficiency at both farm and regional scales, enabling higher application rates where nutrient demand is high whilst simultaneously reducing inputs in areas prone to nutrient surpluses.

Conclusion

This study demonstrated the feasibility of using image analyses to generate plant coverage-based variable N rate recommendations for sown perennial grasslands. However, VRA based on autumn and spring imagery resulted in a better N usage in only one of the two years. Nitrogen responsiveness in temperate forage systems was primarily influenced by interannual weather variability and cut-specific regrowth dynamics, which affected the relative performance of VRA versus fixed high-N strategies. Whilst site-specific manure application offered limited agronomic advantages under conditions of N oversupply, VR approaches consistently maintained yields with substantially lower inputs during years with constrained regrowth, thereby reducing interannual yield and N-use variability compared with fixed strategies. Year-specific differences in overwintering conditions, canopy survival, and illumination-related noise in UAV-derived vegetation indicators likely contributed to variability in autumn- versus spring-derived VR prescriptions, emphasising the need to calibrate cover-based models across a wider gradient of winter severities. Seasonal and climatic differences between years also influenced manure N mineralisation, availability, and the effectiveness of N-rate strategies. Indeed, VRs demonstrated superior resilience under lower-yielding conditions where they more effectively compensated for precipitation variability. Precision N management in perennial forage systems delivers its greatest benefit when rate adjustments are aligned with early-season vigour and declining late-season N responsiveness, whilst also providing a more robust and environmentally efficient nutrient-management framework under variable climatic conditions.

Acknowledgements We would like to thank the technicians at the NIBIO-Særheim research station for carrying out field management and observations.

Author contributions V.P.R-A. and T.P. designed the study, carried out the field experiments and wrote the main manuscript text. V.P.R-A. performed the statistical analyses and prepared all figures, except Fig.2. E.H.C.H. and C.A.R.-A. designed and programmed the Grasision tool and management decision models, prepared Fig. 3, and reviewed the manuscript.

Funding Open access funding provided by Agroscope. This project was funded by the Norwegian Agriculture Agency through Climate and Environment Programme (project number 2021/39760, Agros 163320).

Data availability No datasets were generated or analysed during the current study.

Declarations

Competing interests The authors declare no competing interests.

References

Abadi, M., Barham, P., Chen, J., Chen, Z., Davis, A., Dean, J., Devin, M., Ghemawat, S., Irving, G., Isard, M., Kudlur, M., Levenberg, J., Monga, R., Moore, S., Murray, D. G., Steiner, B., Tucker, P., Vasudevan, V, Warden, P., Wicke, M., Yu, Y., & Zheng, X. (2016). Tensorflow: A system for large-scale machine learning. arXiv preprint arXiv:1605.08695https://doi.org/10.48550/arXiv.1605.08695

AgiSoft (2018) AgiSoft PhotoScan Professional (Version 1.4.5 build 7354) (Software). http://www.agisoft.com/downloads/installer/

Ali, A., Jabeen, N., Farruhbek, R., Chachar, Z., Laghari, A. A., Chachar, S., Ahmed, S., & Yang, Z. (2025). Enhancing nitrogen use efficiency in agriculture by integrating agronomic practices and genetic advances. *Frontiers in Plant Science*. https://doi.org/10.3389/fpls.2025.1543714

Anas, M., Liao, F., Verma, K. K., Sarwar, M. A., Mahmood, A., Chen, Z.-L., Li, Q., Zeng, X.-P., Liu, Y., & Li, Y.-R. (2020). Fate of nitrogen in agriculture and environment: agronomic, eco-physiological and molecular approaches to improve nitrogen use efficiency. *Biological Research 53*(47). https://doi.org/10.1186/s40659-020-00312-4

Argento, F., Anken, T., Abt, F., Vogelsanger, E., Walter, A., & Liebisch, F. (2021). Site-specific nitrogen management in winter wheat supported by low-altitude remote sensing and soil data. *Precision Agriculture, 22*, 364–386. https://doi.org/10.1007/s11119-020-09733-3

Arroyo-Mora, J., Kalacska, M., Løke, T., Schläpfer, D., Coops, N., Lucanus, O., & Leblanc, G. (2021). Assessing the impact of illumination on UAV pushbroom hyperspectral imagery collected under various cloud cover conditions. *Remote Sensing of Environment, 258*, Article 112396. https://doi.org/10.1016/j.rse.2021.112396

Bhogal, A., Williams, J. R., Nicholson, F. A., Chadwick, D. R., Chambers, K. H., & Chambers, B. J. (2016). Mineralization of organic nitrogen from farm manure applications. *Soil Use and Management, 32*(S1), 32–43. https://doi.org/10.1111/sum.12263

Borra-Serrano, I., De Swaef, T., Muylle, H., Nuyttens, D., Vangeyte, J., Mertens, K., Saeys, W., Somers, B., Roldán-Ruiz, I., & Lootens, P. (2019). Canopy height measurements and non-destructive biomass estimation of Lolium perenne swards using UAV imagery. *Grass and Forage Science, 74*(3), 356–369. https://doi.org/10.1111/gfs.12439

Bulacio Fischer, P.T., Carella, A., Massenti, R., Fadhilah, R., & Lo Bianco, R. (2025). Advances in monitoring crop and soil nutrient status: Proximal and remote sensing techniques. *Horticulturae*. https://doi.org/10.3390/horticulturae11020182

Bushong, J. T., Miller, E. C., Raun, W. R., Mullock, J. L., & Arnall, D. B. (2016). Evaluation of mid-season sensor-based nitrogen fertilizer recommendations for winter wheat using different estimates of yield potential. *Precision Agriculture, 17*, 470–494. https://doi.org/10.1007/s11119-016-9431-3

Cameron, K., Di, H., & Moir, J. (2013). Nitrogen losses from the soil/plant system: a review. *Annals of Applied Biology, 162*(2), 145–173. https://doi.org/10.1111/aab.12014

Chapman, D. F., Lee, J. M., Rossi, L., Cosgrove, G. P., Stevens, D. R., Crush, J. R., King, W. M., Edwards, G. R., & Popay, A. J. (2018). Implications of grass-clover interactions in dairy pastures for forage value indexing systems. 1. Context and rationale. New Zealand *Journal of Agricultural Research, 61*(2), 119–146. https://doi.org/10.1080/00288233.2017.1402353

Chen, X., Zhang, H., & Wong, C. U. I. (2025). Dynamic monitoring and precision fertilization decision system for agricultural soil nutrients using UAV remote sensing and GIS. *Agriculture*. https://doi.org/10.3390/agriculture15151627

Chollet, F., and others (2015). Keras. https://keras.io, https://doi.org/10.5281/zenodo.1095037

Congreves, K. A., Otchere, O., Ferland, D., Farzadfar, S., Williams, S., & Arcand, M. M. (2021). Nitrogen use efficiency definitions of today and tomorrow. *Frontiers in Plant Science*. https://doi.org/10.3389/fpls.2021.637108

Gnädinger, F., & Schmidhalter, U. (2017). Digital counts of maize plants by unmanned aerial vehicles (UAVs). *Remote Sensing, 9*, 544. https://doi.org/10.3390/rs9060544

Govindasamy, P., Muthusamy, S. K., Bagavathiannan, M., et al. (2023). Nitrogen use efficiency -a key to enhance crop productivity under a changing climate. *Frontiers in Plant Science*. https://doi.org/10.3389/fpls.2023.1121073

Hagn, L., Mittermayer, M., Kern, A., Kimmelmann, S., Maidl, F.-X., & Hülsbergen, K.-J. (2025). Effects of sensor-based, site-specific nitrogen fertilizer application on crop yield, nitrogen balance, and nitrogen efficiency. *Sensors, 25*(3), 795. https://doi.org/10.3390/s25030795

Helgadóttir, Á., Frankow-Lindberg, B., Seppänen, M. M., Søegaard, K., & Østrem, L. (2014). European grasslands overview: Nordic region. In: Grassland Science in Europe. EGF at 50: The Future of European Grasslands. Proceedings of the 25th General Meeting of the European Grassland Federation, Aberystwyth, Wales, 7–11 September 2014, vol 19. Organising Committee of the 25th General Meeting of the European Grassland Federation, IBERS, 15–28, https://res.slu.se/id/publ/64423

Hnizil, O., Baidani, A., Khlila, I., Nsarellah, N., Laamari, A., & Amamou, A. (2024). Integrating NDVI, spad, and canopy temperature for strategic nitrogen and seeding rate management. *Plants, 13*(11), 1574. https://doi.org/10.3390/plants13111574

Höglind, M., Cameron, D., Persson, T., Huang, X., & van Oijen, M. (2020). Basgra_n: A model for grassland productivity, quality and greenhouse gas balance. *Ecological Modelling, 417*, Article 108925. https://doi.org/10.1016/j.ecolmodel.2019.108925

Jiang, J., Cai, W., Zheng, H., Cheng, T., Tian, Y., Zhu, Y., Ehsani, R., Yongqiang, H., Niu, Q., Gui, L., & Yao, X. (2019). Using Digital Cameras on an Unmanned Aerial Vehicle to Derive Optimum Color Vegetation Indices for Leaf Nitrogen Concentration Monitoring in Winter Wheat. *Remote Sensing, 11*, 2667. https://doi.org/10.3390/rs11222667

Kaim, A., Schmitt, T. M., Annuth, S. H., Haensel, M., & Koellner, T. (2025). An agent-based model to simulate field-specific nitrogen fertilizer applications in grasslands. *European Journal of Agronomy, 165*, Article 127539. https://doi.org/10.1016/j.eja.2025.127539

Kapoor, S., Sood, T., Kaur, J., Hussain, N., & Katoch, V. (2025). Nitrogen nexus: Unraveling the threads of loss, efficiency, and yield. In: Agricultural Nutrient Pollution and Climate Change. Springer Nature, 103–134, https://doi.org/10.1007/978-3-031-80912-5_4

Kataoka, T., Kaneko, T., Okamoto, H., & Hata, S. (2003). Crop growth estimation system using machine vision. In: Proceedings 2003 IEEE/ASME International Conference on Advanced Intelligent Mechatronics (AIM 2003), b1079–b1083, https://doi.org/10.1109/AIM.2003.1225492

King, W., Pletnyakov, P., Taylor, A., Ekanayake, C., & Werner, A. (2022). Variable-rate application of fertiliser - a new tool for farm system and environmental performance? *Journal of New Zealand Grasslands, 83*, 201–213. https://doi.org/10.33584/jnzg.2021.83.3515

Lee, S. W., Swinton, S. M., & Basso, B. (2025). Comparing profitability of variable rate nitrogen prescriptions. Precision Agriculture 26(58). https://doi.org/10.1007/s11119-025-10256-y

Lenth, R. V. (2023). emmeans: Estimated Marginal Means, aka Least-Squares Means. https://CRAN.R-project.org/package=emmeans, r package version 1.8.5

Louro, A., Sawamoto, T., Chadwick, D., Pezzolla, D., Bol, R., Báez, D., & Cardenas, L. (2013). Effect of slurry and ammonium nitrate application on greenhouse gas fluxes of a grassland soil under atypical South West England weather conditions. *Agriculture, Ecosystems & Environment, 181*, 1–11. https://doi.org/10.1016/j.agee.2013.09.005

Miller, J. J., Chanasyk, D. S., Curtis, T. W., & Olson, B. M. (2011). Phosphorus and nitrogen in runoff after phosphorus- or nitrogen-based manure applications. *Journal of Environmental Quality, 40*(3), 949–958. https://doi.org/10.2134/jeq2010.0279

Mitra, B., Singha, P., Chowdhury, A. R., Sinha, A. K., Skalicky, M., Brestic, M., & Hossain, A. (2023). NDVI sensor-based nitrogen management in bread wheat: nutrient uptake, use efficiency, and partial nitrogen balance. *Frontiers in Plant Science, 14*, 1153500. https://doi.org/10.3389/fpls.2023.1153500

Nesme, T., Senthilkumar, K., Mollier, A., & Pellerin, S. (2015). Effects of crop and livestock segregation on phosphorus resource use: A systematic, regional analysis. *European Journal of Agronomy, 71*, 88–95. https://doi.org/10.1016/j.eja.2015.08.001

Pawase, P. P., Nalawade, S. M., Bhanage, G. B., Walunj, A. A., Kadam, P. B., Durgude, A. G., & Patil, M. G. (2023). Variable rate fertilizer application technology for nutrient management: A review. *International Journal of Agricultural and Biological Engineering, 16*(4), 11–19. https://doi.org/10.25165/j.ijabe.20231604.7671

Persson, T., Murguzur, F. J. A., Davids, C., Höglind, M., & Jørgensen, M. (2024). Combining satellite-sensed and ground data and the basgra model to predict grass yield in high-latitude regions. *Field Crops Research, 318*, Article 109610. https://doi.org/10.1016/j.fcr.2024.109610

Peters, T., Kluß, C., Vogeler, I., Loges, R., Fenger, F., & Taube, F. (2022). Grasprog: Pasture model for predicting daily pasture growth in intensive grassland production systems in northwest europe. *Agronomy*. https://doi.org/10.3390/agronomy12071667

Pinheiro, J., Bates, D., R Core Team (2023). nlme: Linear and Nonlinear Mixed Effects Models. https://CRAN.R-project.org/package=nlme, r package version 3.1-162

Pinto, J. C., Arnall, B., & Puntel, L. A. (2025). Evaluation of static and sensor-based nitrogen recommendation models for winter wheat. *Agronomy Journal*. https://doi.org/10.1002/agj2.70063

QGIS Development Team (2025) QGIS Geographic Information System, Version 3.40. Open Source Geospatial Foundation, https://doi.org/10.5281/zenodo.16881931, https://qgis.org

R Core Team (2025) R: A Language and Environment for Statistical Computing. R Foundation for Statistical Computing, Vienna, Austria, https://www.R-project.org/

Rapacz, M., Ergon, Å., Höglind, M., Jørgensen, M., Jurczyk, B., Østrem, L., Rognli, O. A., & Tronsmo, A. M. (2014). Overwintering of herbaceous plants in a changing climate. still more questions than answers. *Plant Science, 225*, 34–44. https://doi.org/10.1016/j.plantsci.2014.05.009

Rasmussen, J., Ntakos, G., Nielsen, J., Svensgaard, J., Poulsen, R., & Christensen, S. (2016). Are vegetation indices derived from consumer-grade cameras mounted on UAVs sufficiently reliable for assessing experimental plots? *European Journal of Agronomy, 74*, 75–92. https://doi.org/10.1016/j.eja.2015.11.026

Raun, W. R., & Johnson, G. V. (1999). Improving nitrogen use efficiency for cereal production. *Agronomy Journal, 91*(3), 357–363. https://doi.org/10.2134/agronj1999.00021962009100030001x

Reuter, T., Nahrstedt, K., Jarmer, T., Broll, G., Dieter TrautzReuter, T., Nahrstedt, K., Jarmer, T., et al. (2025). Delineation of management zones in clover-grass for site-specific management of subsequent crops. *Precision Agriculture, 26*(4), 61. https://doi.org/10.1007/s11119-025-10260-2

Roth, L., & Streit, B. (2017). Predicting cover crop biomass by lightweight UAS-based RGB and NIR photography: an applied photogrammetric approach. *Precision Agriculture, 19*, 93–114. https://doi.org/10.1007/s11119-017-9501-1

Rueda-Ayala, C. A., Rueda-Ayala, V. P., Höglind, M., & Andújar, D. (2019). Accurate segmentation of grass-sward structures in RGB images using machine learning algorithms. Wageningen Academic PublishersIn E. van Henten, D. Goense, & C. Lokhorst (Eds.), *Precision Agriculture '19, 12th European Conference on Precision Agriculture (ECPA)* (Vol. 12, pp. 623–627). The Netherlands: Wageningen.

Rueda-Ayala, V. P., Peña, J. M., Höglind, M., Bengochea-Guevara, J. M., & Andújar, D. (2019). Comparing uav-based technologies and RGB-D reconstruction methods for plant height and biomass monitoring on grass ley. *Sensors, 19*(3), 535. https://doi.org/10.3390/s19030535

Rueda-Ayala, V. P., & Höglind, M. (2019). Determining thresholds for grassland renovation by sod-seeding. *Agronomy, 9*(12), 86–94. https://doi.org/10.3390/agronomy9120842

Schoumans, O. F., Chardon, W. J., Bechmann, M. E., Gascuel-Odoux, C., Hofman, G., Kronvang, B., Rubæk, G. H., Ulén, B., & Dorioz, J.-M. (2014). Mitigation options to reduce phosphorus losses from the agricultural sector and improve surface water quality: A review. *Science of The Total Environment, 468–469*, 1255–1266. https://doi.org/10.1016/j.scitotenv.2013.08.061

Shingfield, K., Jaakkola, S., & Huhtanen, P. (2001). Effects of level of nitrogen fertilizer application and various nitrogenous supplements on milk production and nitrogen utilization of dairy cows given grass silage-based diets. *Animal Science, 73*(3), 541–554. https://doi.org/10.1017/S1357729800058513

Sigua, G. C., Williams, M. M., Jr, C., Chad, C., Grabowski, J., & Kongchum, M. (2013). Nitrogen recovery and agronomic efficiency of forages with nitrogen fertilization under flooded condition. *Agricultural Sciences,4*, 163–173. https://doi.org/10.4236/as.2013.43021

Silva, L., Conceição, L. A., Lidon, F. C., & Maçãs, B. (2023). Remote monitoring of crop nitrogen nutrition to adjust crop models: A review. *Agriculture*. https://doi.org/10.3390/agriculture13040835

Silvestri, N., Ercolini, L., Grossi, N., & Ruggeri, M.(2024). Integrating NDVI and agronomic data to optimize the variable-rate nitrogen fertilization. *Precision Agriculture, 25*, 2554–2572. https://doi.org/10.1007/s11119-024-10185-2

Smit, H. P. J., Reinsch, T., Kluß, C., Loges, R., & Taube, F. (2021). Very low nitrogen leaching in grazed ley-arable-systems in northwest europe. *Agronomy*. https://doi.org/10.3390/agronomy11112155

Stamatiadis, S., Schepers, J. S., Evangelou, E., Tsadilas, C., Glampedakis, A., Glampedakis, M., Dercas, N., Spyropoulos, N., Dalezios, N. R., & Eskridge, K. (2018). Variable-rate nitrogen fertilization of winter wheat under high spatial resolution. *Precision Agriculture, 19*, 570–587. https://doi.org/10.1007/s11119-017-9540-7

Sun, X., Luo, N., Longhurst, B., & Luo, J. (2008). Fertiliser nitrogen and factors affecting pasture responses. *The Open Agriculture Journal, 2*, 35–45. https://doi.org/10.2174/1874331500802010035

Svanbäck, A., McCrackin, M. L., Swaney, D. P., Linefur, H., Gustafsson, B. G., Howarth, R. W., & Humborg, C. (2019). Reducing agricultural nutrient surpluses in a large catchment - links to livestock density. *Science of The Total Environment, 648*, 1549–1559. https://doi.org/10.1016/j.scitotenv.2018.08.194

Termonen, M., Korhonen, P., Kykkanen, S., Karkonen, A., Toivakka, M., Kauppila, R., & Virkajarvi, P. (2020). Effects of nitrogen application rate on productivity, nutritive value and winter tolerance of timothy and meadow fescue cultivars. *Grass and Forage Science, 75*(1), 111–126. https://doi.org/10.1111/gfs.12461

Valkama, E., Rankinen, K., Virkajärvi, P., Salo, T., Kapuinen, P., & Turtola, E. (2016). Nitrogen fertilization of grass leys: Yield production and risk of n leaching. *Agriculture, Ecosystems & Environment, 230*, 341–352. https://doi.org/10.1016/j.agee.2016.05.022

Vizzari, M., Santaga, F., & Benincasa, P. (2019). Sentinel-2-based nitrogen VRT fertilization in wheat: comparison between traditional and simple precision practices. *Agronomy, 9*(6), 278. https://doi.org/10.3390/agronomy9060278

Wachendorf, M., Büchter, M., Trott, H., & Taube, F. (2004). Performance and environmental effects of forage production on sandy soils. ii. impact of defoliation system and nitrogen input on nitrate leaching losses. *Grass and Forage Science, 59*(1), 56–68. https://doi.org/10.1111/j.1365-2494.2004.00401.x

Zhang, J., Guerrero, A., & Mouazen, A. M. (2022). Simulation of variable-rate manure application under different application scenarios. *Soil and Tillage Research, 221*, Article 105416. https://doi.org/10.1016/j.still.2022.105416

Zhang, J., Borundia, A., & Mouazen, A. M. (2024). Map-sensor-based site-specific manure application in wheat. *Computers and Electronics in Agriculture, 219*, Article 108764. https://doi.org/10.1016/j.compag.2024.108764

Zhang, J., Sleutel, S., & Mouazen, A. M. (2024). Phosphorus-based variable rate manure application in wheat and barley. *Precision Agriculture, 25*, 1714–1730. https://doi.org/10.1007/s11119-024-10131-2

Authors and Affiliations

Victor Rueda-Ayala[1] · Tomas Persson[2] · El Houssein Chouaib Harik[3] · Christian Rueda-Ayala[4]

✉ Victor Rueda-Ayala
patovicnsf@gmail.com

Tomas Persson
tomas.persson@nibio.no

El Houssein Chouaib Harik
chouaib.harik@sintef.no

Christian Rueda-Ayala
christian.rueda@csic.es

1 Weed Science in Field Crops, Agroscope, Route de Duillier 60, Nyon 1260, Switzerland

2 Livestock and Forage, Norwegian Institute of Bioeconomy Research (NIBIO), Postboks 11, 1431 Ås, Norway

3 Production Technology, Robotics and Automation, SINTEF Manufacturing AS, Grøndalsvegen 2, 2830 Raufoss, Norway

4 Instituto Nacional de Investigación y Tecnología Agraria y Alimentaria (INIA), Consejo Superior Investigaciones Científicas (CSIC), Carretera de la Coruña, km 7.5, Madrid 28040, Spain